Supplementary Section

Unveiling dye adsorption capability of *Moringa oleifera* functionalized hybrid porous MOF-GO composites: *In vitro* and *in silico* ecotoxicity assessment via antibacterial and molecular docking studies

Graphene oxide (GO) characterization

The textural properties of GO were analyzed using SEM imaging (Fig. S1a). The representative image depicts a 2D morphology of GO with crumpled and folded textures characterized by rough surfaces and irregular edges. The composition of GO analyzed by EDS spectra confirms the presence of carbon (C) and oxygen (O) elements with an atomic percentage of 66.84 and 33.14%, respectively (Fig. S1b).

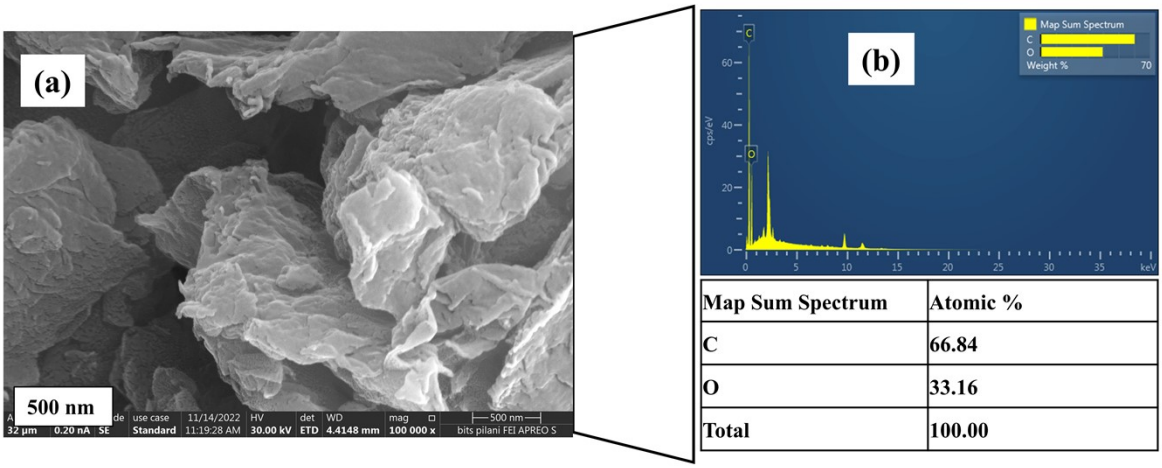

Map Sum Spectrum	Atomic %
C	66.84
O	33.16
Total	100.00

Fig. S1 Micrographs of (a) SEM GO and (b) EDS spectra of GO.

Fig. S2 represents the recorded XRD patterns and FTIR spectra of as-prepared GO. The representative XRD pattern of synthesized GO has been shown in Fig. S2a. The peaks at 2θ values of 10.52 and 42.5 correspond to (002) and (001) planes, respectively. The obtained patterns precisely match with existing patterns of GO from the literature studies [1–4]. The obtained characteristic peak of GO demonstrated the high purity with an interplanar spacing distance of ~0.85 nm, which is best suited for possible combination with the MOF materials. The FTIR analysis showed broad, sharp spectra located at 3414 cm^{-1} corresponding to the O–H stretching vibration, which indicates the presence of hydroxyl (–OH) and carboxylic functional (–COOH) groups within the GO structure (Fig. S2b). The peaks observed at 1719 and 1050 cm^{-1} were due to stretching vibrations of carbonyl (C=O) and epoxy (C–O) groups, respectively. The peak at 1614 cm^{-1} was mainly due to the stretching of unoxidized graphite

present in the sample. The presence of functional groups, including hydroxyl, carboxyl, carbonyl, and epoxy, analyzed in the current sample (GO) aligns with findings from previous literature studies [5,6]. These results affirm the success of the experimental employment of Hummer's method in oxidizing graphite into GO. Furthermore, these findings also provide more evidence in favor of the prospective use of the produced GO in combination with MOF materials.

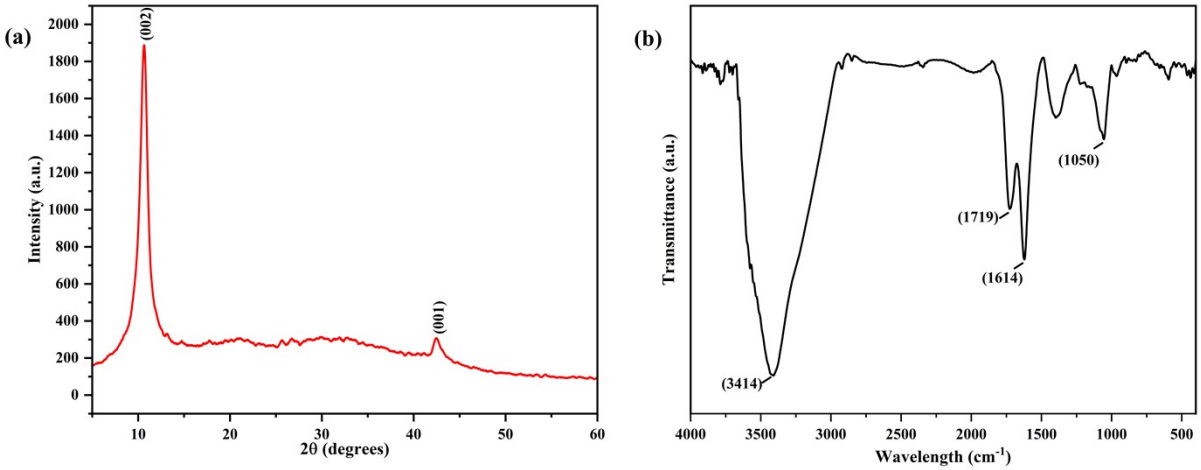

Fig. S2 Recorded spectra of GO from (a) XRD and (b) FTIR.

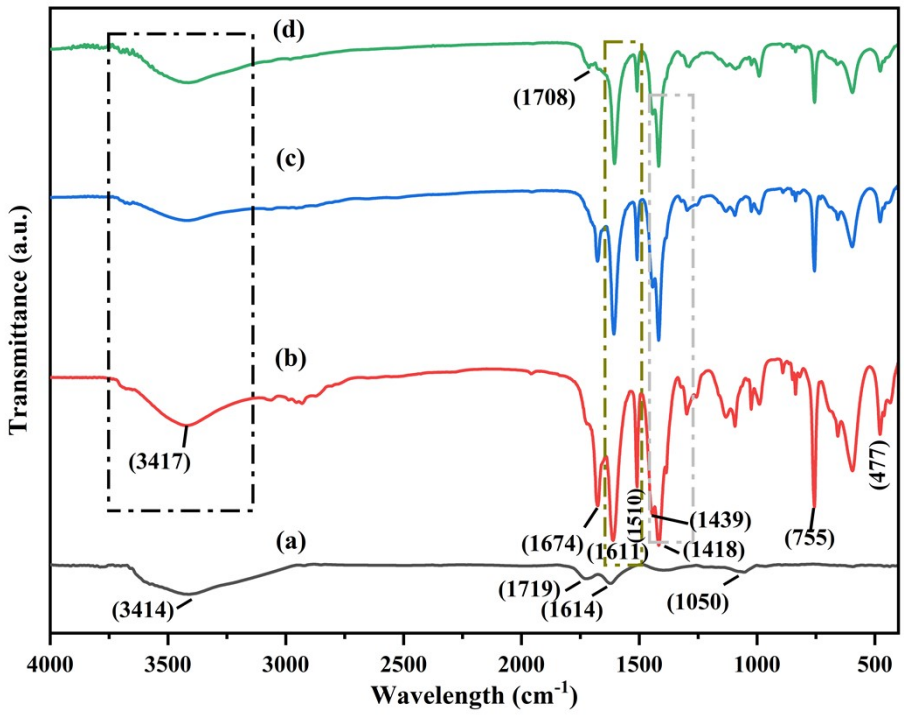

Fig. S3 FTIR spectra of (a) GO, (b) Al-MOF, (c) AlG, and (d) AlGC.

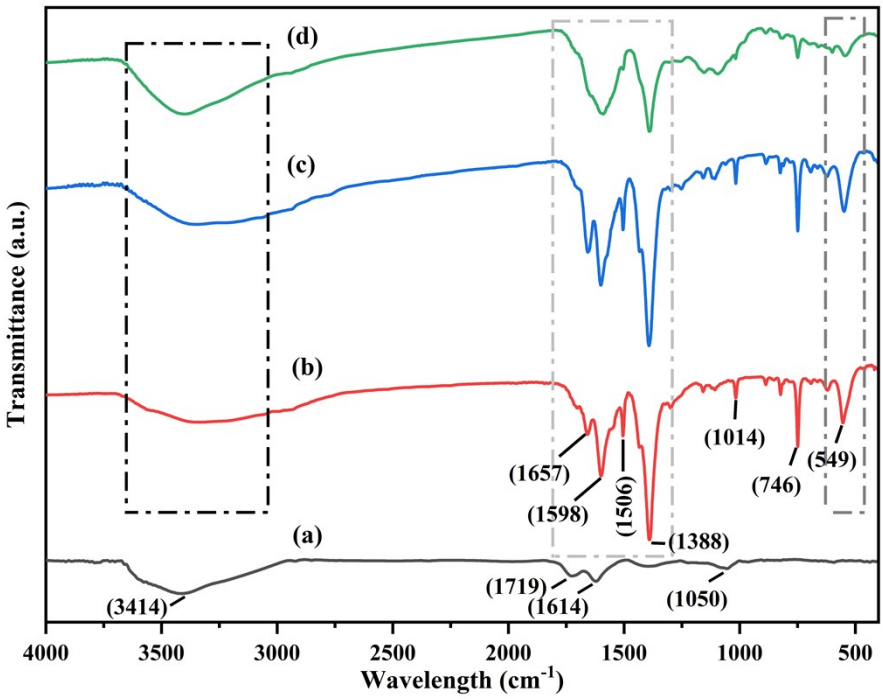

Fig. S4 FTIR spectra of (a) GO, (b) Fe-MOF, (c) FeG, and (d) FeGC.

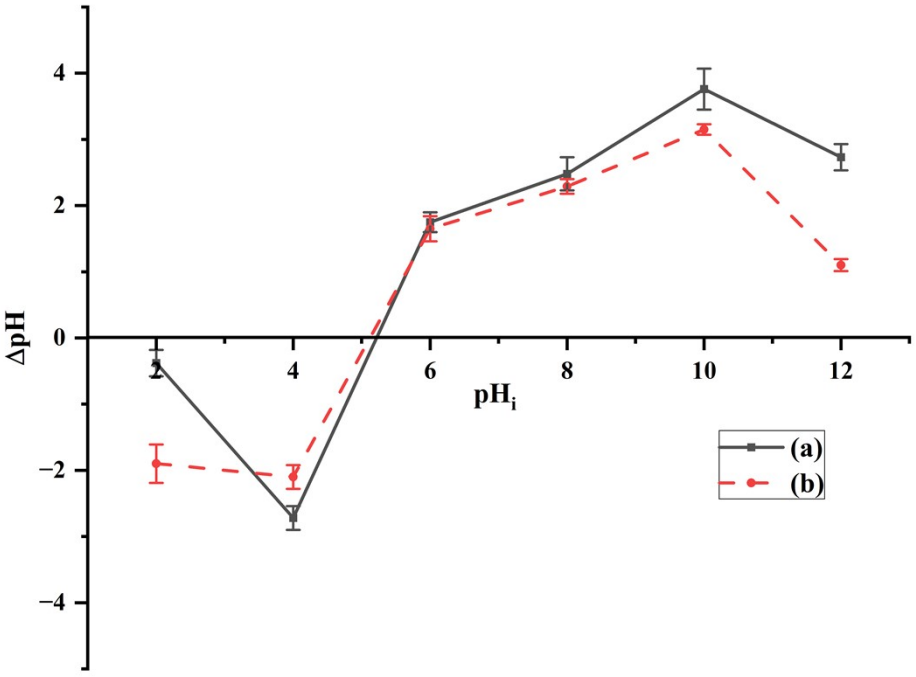

Fig. S5 Surface charge analysis for the composite (a) AlGC and (b) FeGC.

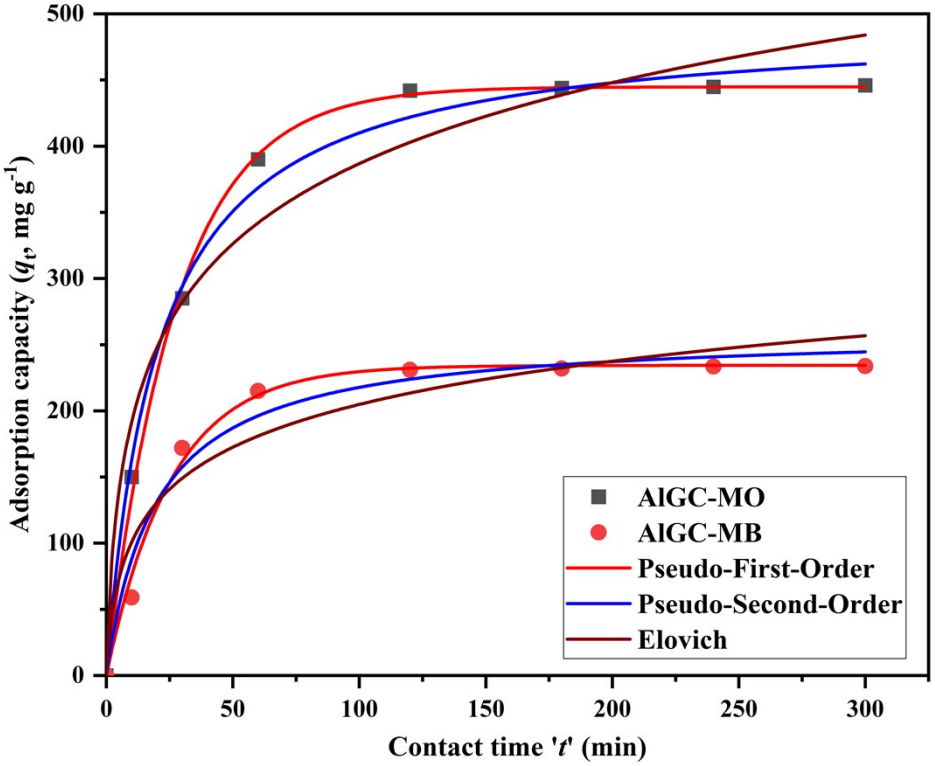

Fig. S6 Kinetic models non-linear fitting for removing MO & MB adsorption using AlGC composite.

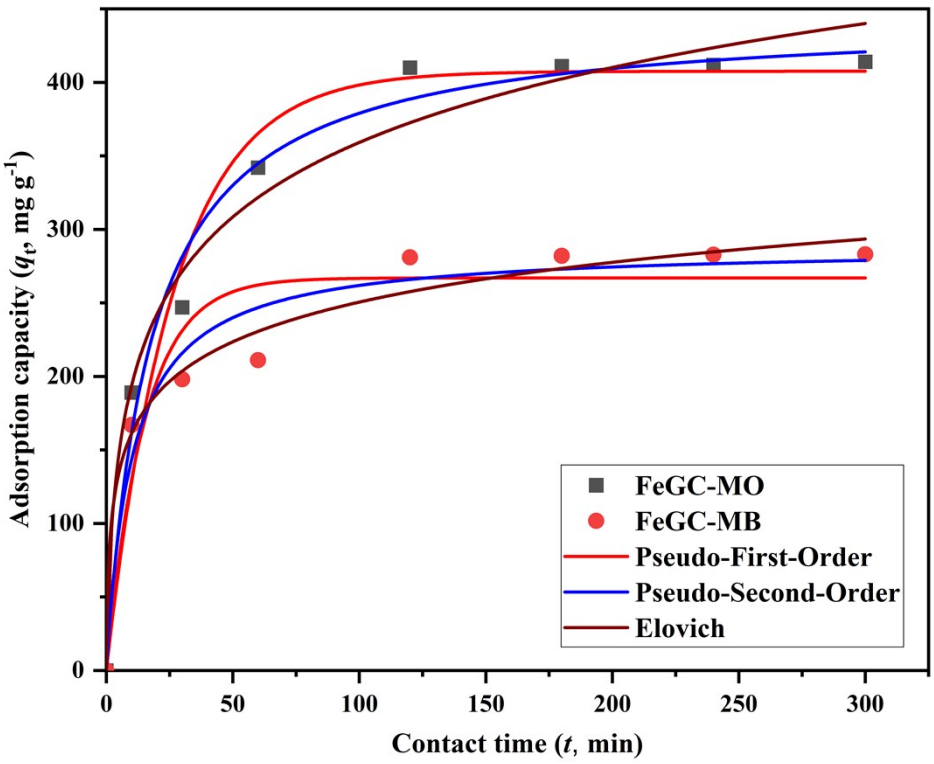

Fig. S7 Kinetic models non-linear fitting for removing Mo & MB adsorption using FeGC composite.

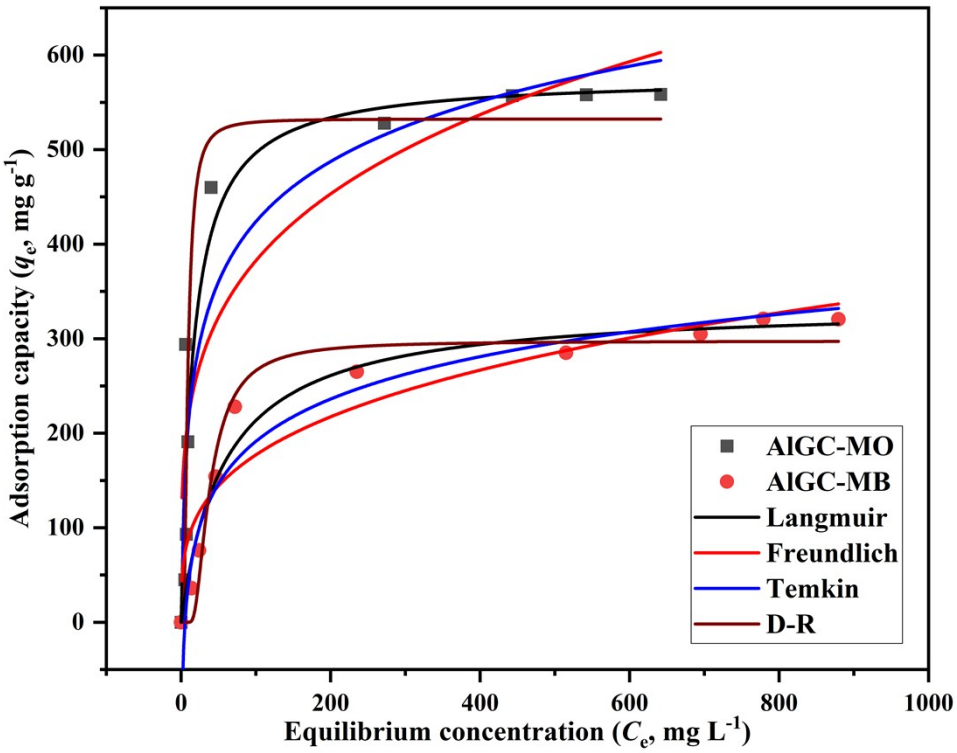

Fig. S8 Applicability of different isotherm models for MO & MB removal using AlGC composite.

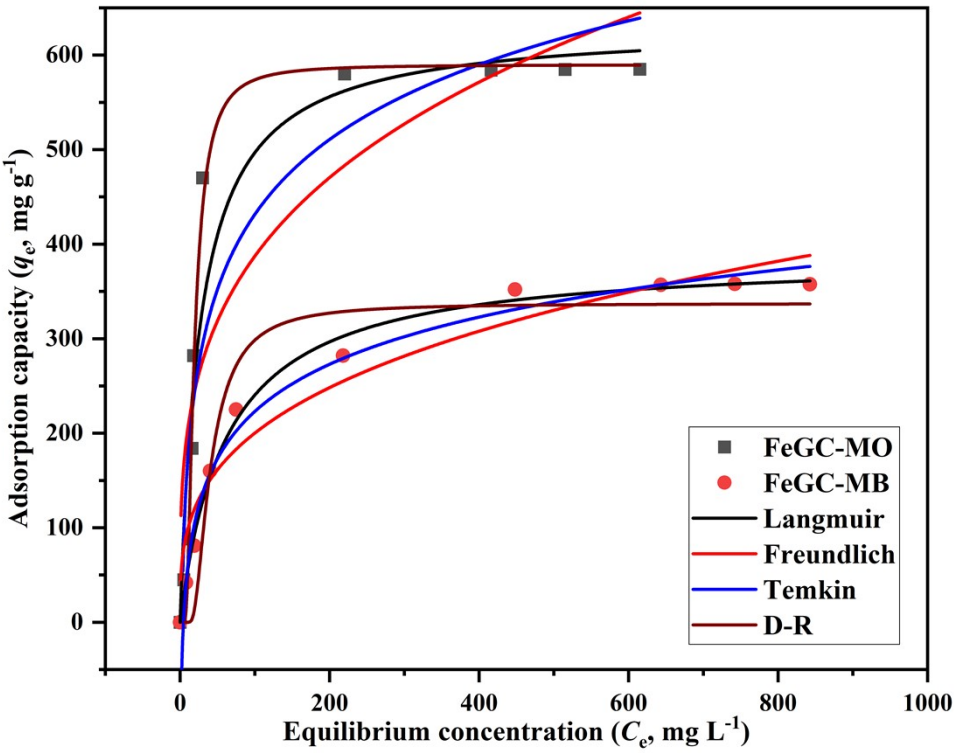

Fig. S9 Applicability of different isotherm models for MO & MB removal using FeGC composite.

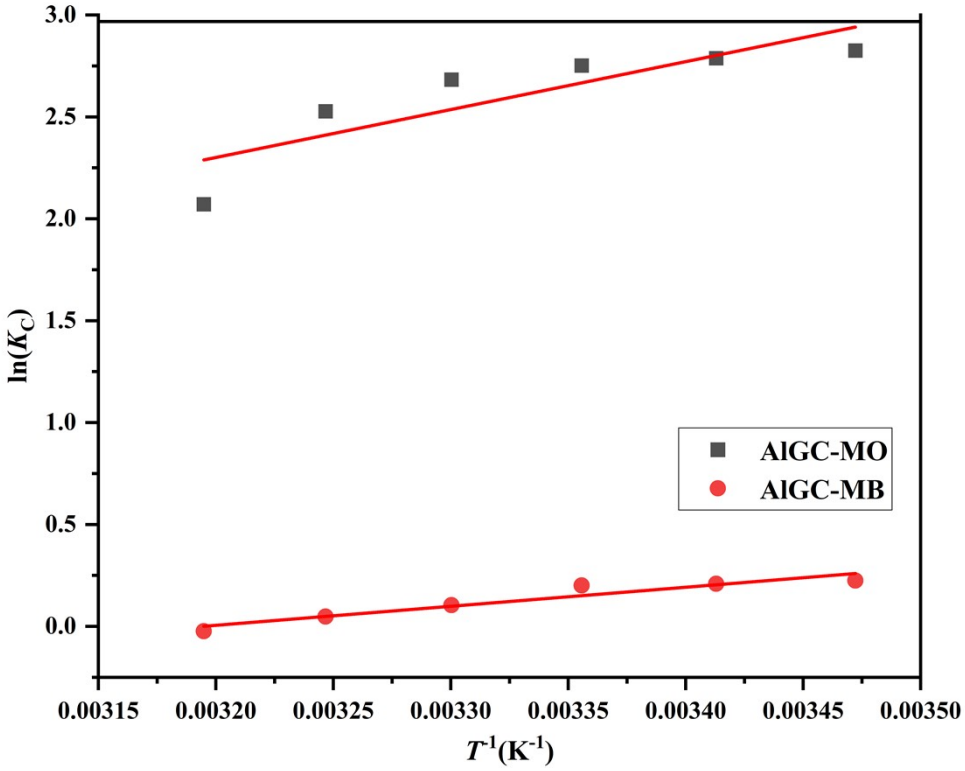

Fig. S10 Van't Hoff linear fit for thermodynamic data for the MO & MB adsorption using AlGC composites.

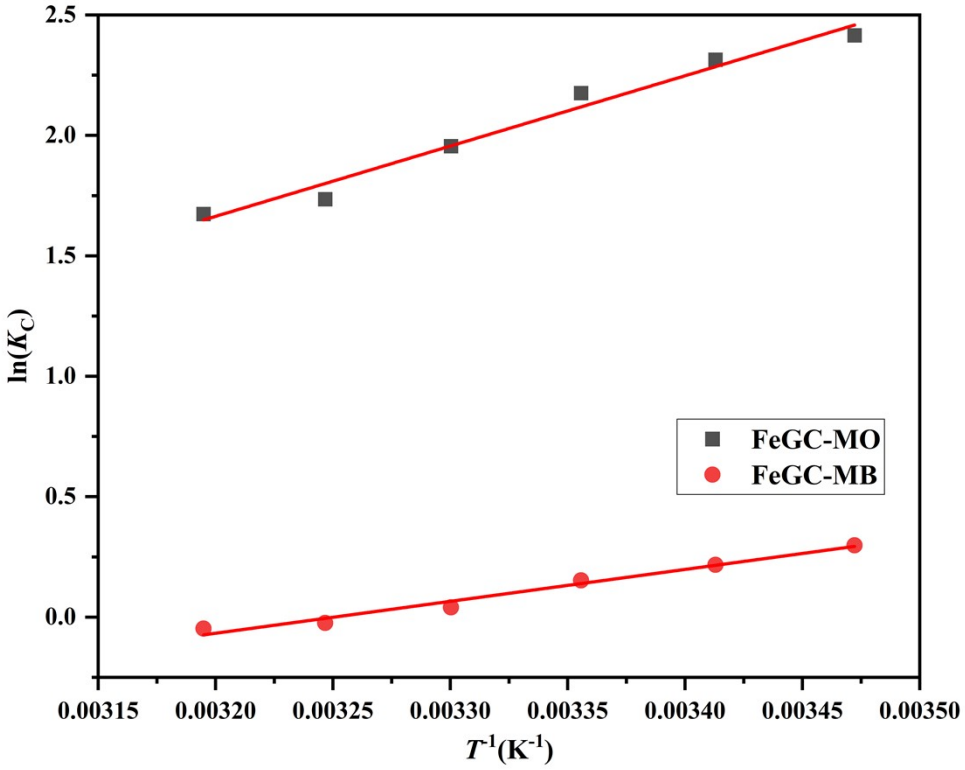

Fig. S11 Van't Hoff linear fit for thermodynamic data for the MO & MB adsorption using FeGC composites.

Table S1 L25 orthogonal array approach was used for the optimization process.

Experiment	Factor A	Factor B	Factor C	Factor D
1	1	1	1	1
2	1	2	2	2
3	1	3	3	3
4	1	4	4	4
5	1	5	5	5
6	2	1	2	3
7	2	2	3	4
8	2	3	4	5
9	2	4	5	1
10	2	5	1	2
11	3	1	3	5
12	3	2	4	1
13	3	3	5	2
14	3	4	1	3
15	3	5	2	4
16	4	1	4	2
17	4	2	5	3
18	4	3	1	4
19	4	4	2	5
20	4	5	3	1
21	5	1	5	4
22	5	2	1	5
23	5	3	2	1
24	5	4	3	2
25	5	5	4	3

Table S2 Experimental design matrix with a response for MO & MB removal using AlGC and FeGC composite.

					AlGC				FeGC			
					MO		MB		MO		MB	
S. No.	Time (min)	Mass (mg)	Conc. (mg L^{-1})	Temp. (°C)	Q (mg g^{-1})	S/N	Q (mg g^{-1})	S/N	Q (mg g^{-1})	S/N	Q (mg g^{-1})	S/N
1	10	10	100	20	120.39	41.61	118	41.44	86.43	38.73	74	37.38
2	10	15	200	25	205.79	46.27	146.67	43.33	191.38	45.64	135	42.61
3	10	20	300	30	277.81	48.87	171	44.66	259.29	48.28	165	44.35
4	10	25	400	35	266.7	48.52	164	44.3	248.18	47.9	147	43.35
5	10	30	500	40	217.11	46.73	202.67	46.14	275.75	48.81	216	46.69
6	30	10	200	30	376.59	51.52	228	47.16	327.2	50.3	228	47.16
7	30	15	300	35	364.24	51.23	186.67	45.42	281.93	49	170	44.61
8	30	20	400	40	169.77	44.6	152	43.64	274.73	48.78	141	42.98
9	30	25	500	20	371.65	51.4	193.6	45.74	328.44	50.33	175	44.86
10	30	30	100	25	80.42	38.11	60	35.56	83.22	38.4	62	35.85
11	60	10	300	40	305.51	49.7	189	45.53	330.29	50.38	228	47.16
12	60	15	400	20	395	51.93	258.67	48.25	388.94	51.8	248	47.89
13	60	20	500	25	384.56	51.7	245	47.78	364.24	51.23	240	47.6
14	60	25	100	30	64.21	36.15	67.2	36.55	64.69	36.22	71.2	37.05
15	60	30	200	35	129.65	42.26	118.67	41.49	126.56	42.05	118	41.44
16	120	10	400	25	378.49	51.56	246	47.82	395.11	51.93	254	48.1
17	120	15	500	30	390.62	51.84	272	48.69	410.85	52.27	265	48.46
18	120	20	100	35	81.8	38.26	89	38.99	82.48	38.33	86	38.69
19	120	25	200	40	111.12	40.92	145.6	43.26	128.41	42.17	138.4	42.82
20	120	30	300	20	180.06	45.11	176	44.91	163.6	44.28	144	43.17
21	180	10	500	35	367.33	51.3	252	48.03	405.88	52.17	216	46.69
22	180	15	100	40	96.72	39.71	44.5	32.97	74.08	37.39	66.1	36.4
23	180	20	200	20	162.06	44.19	161	44.14	163.68	44.28	128	42.14
24	180	25	300	25	230.89	47.27	193.6	45.74	208.67	46.39	148.8	43.45
25	180	30	400	30	255.18	48.14	192	45.67	247.97	47.89	123.33	41.82

Table S3 ANOVA for the adsorption capacity of AlGC and FeGC.

Adsorbent- AlGC for MO						
Source	DF	Adj SS	Adj MS	F-Value	P-Value	% Contribution
Regression	4	262385	65596	21.83	0	
Time	1	1731	1731	0.58	0.457	0.53
Mass	1	63338	63338	21.08	0	19.6
Conc	1	186708	186708	62.14	0	57.89
Temp	1	10608	10608	3.53	0.075	3.28
Error	20	60089	3004			
Total	24	322474				
r^2				77.64%		
Adsorbent- AlGC for MB						
Regression	4	78046.8	19511.7	23.05	0	
Time	1	463.6	463.6	0.55	0.468	0.48
Mass	1	10134	10134	11.97	0.002	10.67
Conc	1	63786.6	63786.6	75.37	0	67.16
Temp	1	3662.5	3662.5	4.33	0.051	3.85
Error	20	16927.4	846.4			
r^2				78.61%		
Adsorbent- FeGC for MO						
Regression	4	288748	72187	49.42	0	
Time	1	549	549	0.38	0.547	0.17
Mass	1	55405	55405	37.93	0	17.42
Conc	1	232047	232047	158.85	0	72.97
temp	1	747	747	0.51	0.483	0.23
Error	20	29216	1461			
r^2				88.97%		
Adsorbent- FeGC for MB						
Regression	4	71562.3	17890.6	15.15	0	
Time	1	235.1	235.1	0.2	0.66	0.24
Mass	1	15384	15384	13.03	0.002	16.16
Conc	1	55866.9	55866.9	47.3	0	58.69
Temp	1	76.4	76.4	0.06	0.802	0.08
Error	20	23621.1	1181.1			
Total	24	95183.4				
r^2				75.18%		

References

1 S. D. Perera, R. G. Mariano, K. Vu, N. Nour, O. Seitz, Y. Chabal and K. J. Balkus, *ACS Catalysis*, 2012, **2**, 949–956.

2 A. Giménez-Pérez, S. K. Bikkarolla, J. Benson, C. Bengoa, F. Stüber, A. Fortuny, A. Fabregat, J. Font and P. Papakonstantinou, *Journal of Materials Science*, 2016, **51**, 8346–8360.

3 M. Lu, L. Li, S. Shen, D. Chen and W. Han, *New Journal of Chemistry*, 2019, **43**, 1032–1037.

4 T. Chowdhury, L. Zhang, J. Zhang and S. Aggarwal, *Materials Advances*, 2021, **2**, 3051–3059.

5 R. A. Rochman, S. Wahyuningsih, A. H. Ramelan and Q. A. Hanif, *IOP Conference Series: Materials Science and Engineering*, 2019, **509**, 012119.

6 M. Bera, Chandravati, P. Gupta and P. K. Maji, *Journal of Nanoscience and Nanotechnology*, 2018, **18**, 902–912.